

ON LEPTON PAIR PRODUCTION IN PROTON–ANTIPROTON COLLISIONS AT INTERMEDIATE ENERGIES

A. N. Skachkova, N. B. Skachkov

Joint Institute for Nuclear Research, Dubna

The lepton pair production via the quark–antiquark annihilation subprocess in collisions of beam antiproton with the proton target at $E_{\text{beam}} = 14$ GeV is studied on the basis of the event sample simulated by PYTHIA6 generator. Different kinematical variables which may be useful for the design of the muon system and the electromagnetic calorimeter of the detector of PANDA experiment at FAIR, as well as for the study of proton structure functions in the available $x-Q^2$ kinematical region, are considered. It is also argued that the measurement of the total transverse momentum of a lepton–antilepton system may provide important information about the intrinsic transverse momentum $\langle k_T \rangle$ that appears due to the Fermi motion of quarks inside the nucleon. Another interesting possibility is the measurement of the production rate of two or three lepton pairs in one event that can give the information about the rate of multiple quarks interactions and the proton space structure. The problems due to the presence of fake leptons that appear from meson decays, as well as due to the contribution of background QCD processes and minimum bias events, are also discussed. The set of cuts which allows one to separate the events with the signal lepton pairs from different kind of background events is proposed.

Процесс рождения лептонных пар в результате кварк–антикваркового взаимодействия (аннигиляции) в столкновениях антипротонных пучков при энергии 14 ГэВ с протонной мишенью изучен на основе событий, смоделированных с помощью генератора PYTHIA6. Рассмотрены различные кинематические переменные, которые могут быть полезны для проектирования мюонной системы и электромагнитного калориметра для детектора эксперимента PANDA на FAIR, а также для изучения структурных функций протона в доступной $x-Q^2$ кинематической области. Также показано, что измерение полного поперечного импульса лептон–антилептонной системы как целого может предоставить важную информацию о внутреннем поперечном импульсе $\langle k_T \rangle$, возникающем вследствие ферми-движения кварков внутри нуклона. Другая интересная возможность — измерение выхода двух или трех лептонных пар в одном событии, которое дает информацию о доле множественных взаимодействий и пространственной структуре протона. Также рассмотрена проблема присутствия фоновых лептонов, появляющихся как в результате распадов мезонов, так и за счет вклада фоновых КХД и minimum bias процессов. Предложен ряд критериев, позволяющих отделить сигнальные события с лептонными парами от фоновых событий.

PACS: 12.38.Qk; 13.85.Fb; 13.85.Qk

INTRODUCTION

The measurements of lepton pair production in strong hadron–hadron interactions (see [1] and [2]) have already demonstrated their great potential for studying the properties of elementary particles. As for illustration, it is enough to mention the facts of discovery of charmed

$J(J/\Psi)$ as well as of beauty Υ mesons which were done first in hadron–hadron collisions and confirmed later in e^+e^- experiments. Dilepton events may serve as a powerful tool to get out the information about the parton distribution functions (PDF) in hadrons as it was already shown in a number of high energy experiments [3] and theoretical papers, devoted to the data analysis in the framework of QCD [4]. The plans to study this process are included into the TPR [5] of PANDA experiment at HESR which may provide an interesting information about quark dynamics inside the nucleon.

This intermediate energy experiment (in the following we shall consider the case of antiproton beam energy $E_{\text{beam}} = 14$ GeV which corresponds to the center-of-mass energy of the $p\bar{p}$ system $E_{\text{cm}} = 5.3$ GeV) may play an important role because it allows one to study the energy range where the perturbative methods of QCD (pQCD) come into interplay with a rich physics of bound states and resonances. The physics of hadron resonances formation and decay is strongly connected with the confinement problem, i.e., with the parton dynamics at large distances. Therefore, a detailed and high-precision experimental study of lepton pair production at PANDA may allow one to discriminate between a large variety of existing nonperturbative approaches and models that already exist or under development now.

To reach the goals declared in [5], a reasonable modeling of energy-momentum and angle distributions of the produced lepton pairs has to be done. Such a sort of Monte-Carlo simulation of $\bar{p}p \rightarrow l^+l^- + X$ process [6] (see Fig. 1) is also needed for the design of the muon system and electromagnetic calorimeter. We utilized here, as for the first step, the PYTHIA event generator [7], which is based on the ideas of the quark parton model and is well tested and widely used for simulation of hadron–hadron interactions. To define the cross sections of processes, PYTHIA uses the perturbative QCD/QED amplitude of the $q\bar{q} \rightarrow l^+l^-$ subprocess which provides a proper account of the relativistic kinematics during simulation of different physical variables distributions specific for $\mu^+\mu^-$ - or e^+e^- -pair production.

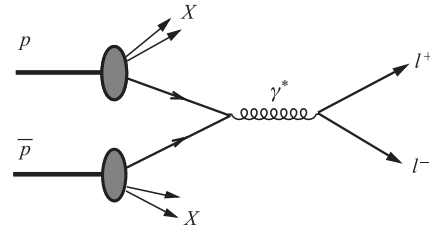


Fig. 1. $\bar{p}p \rightarrow l^+l^- + X$ process

Let us underline that the results obtained here on the basis of PYTHIA simulation in some sense may allow one to fix the predictions for lepton kinematical distributions which may be obtained in the framework of perturbative theory approach. Therefore, they may be useful at the analysis stage for defining the boundary between nonperturbative and perturbative models predictions.

In Sec. 1 we present the kinematical distributions for individual leptons. The set of plots with energy, transverse momentum and angle distributions are given together with some «3-dimensional plots» which show different kinds of correlations (like Energy–Energy, Energy–Angle and Angle–Angle correlations) between the physical variables of leptons produced via the quark level subprocess $q\bar{q} \rightarrow l^+l^-$.

In Sec. 2 we present the distribution of the invariant mass and some other physical variables which are characteristic for the signal lepton pair as a whole system.

The problems connected with the background from fake leptons which may appear together with the signal lepton pair in one and the same event due to meson decays as well as with the

background from other than $q\bar{q} \rightarrow l^+l^-$ subprocess are discussed in Sec. 3. Also we present a set of cuts which allows one to separate the background events from the signal ones. The efficiencies of the proposed cuts are also given.

In Sec. 4 we outline some important physical measurements which can be done by studying the lepton pair production at the energies available for PANDA experiment.

It is worth mentioning that the results presented here can also be useful for the future physical analysis of hadron decays at PANDA because the contribution from $p\bar{p} \rightarrow l^+l^- + X$ events may be one of the main background sources in such a study.

1. DISTRIBUTIONS OF LEPTONS PRODUCED IN $p\bar{p}$ COLLISIONS

We use PYTHIA6 to generate 100 000 $\langle p\bar{p} \rightarrow l^+l^- + X \rangle$ events which include the $2 \rightarrow 2$ quark level $q\bar{q} \rightarrow \gamma^* \rightarrow l^+l^-$ subprocess. In the following, these events will be called «signal events», and the muons/electrons produced in this subprocess will be called «signal» leptons. The fake leptons which are produced in hadron (mainly mesons) decays in the same signal events will be called «decay» leptons. The simulation is done starting from the assumption of the ideal muon system and electromagnetic calorimeter covering 360° .

We consider the case where both initial-state radiation (ISR) and final-state radiation (FSR) were switched on simultaneously¹; i.e., the corresponding PYTHIA parameters were used. Also we have used the CTEQ2L parametrization of parton distributions and the default value of the parameter, which allows one to take into account the primordial k_T -effect (the effect of quark Fermi motion inside the hadron).

First we consider the distributions of some physical variables which describe the kinematics of individual leptons belonging to the l^+l^- pair. Simulation shows that there is no difference between e^+e^- and $\mu^+\mu^-$ distributions. In all the following figures, except Figs. 5 and 6, the vertical axis shows the number of events (per bin) that may be expected per year (10^7 s) for the luminosity $L = 2 \cdot 10^{32} \text{ cm}^{-2} \cdot \text{s}^{-1}$. The total number of expected events is shown as «Integral» values in the figures.

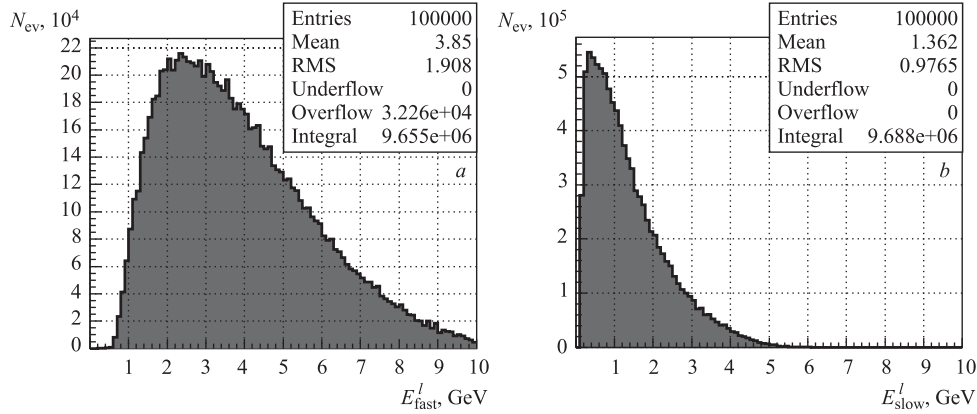


Fig. 2. Distribution of number of signal events versus the energy of signal leptons. *a*) The energy of fast leptons E_{fast}^l ; *b*) the energy of slow leptons E_{slow}^l

¹This fact would be important for the discussion in Sec. 3.

Figure 2 includes the set of plots done separately for the signal leptons having the largest energy E_{fast}^l in the lepton pair and for the leptons having a smaller energy E_{slow}^l in the pair. We shall call them, correspondingly, «fast» (plot *a*) and «slow» (plot *b*) leptons. One can see that the energy spectrum of the fast signal leptons (plot *a*) increases rather fast from the point $E_{\text{fast}}^l \approx 0.5$ GeV (more than 90% of fast leptons have $E_{\text{fast}}^l > 1$ GeV) up to the peak position at the point $E_{\text{fast}}^l \approx 2.5$ GeV and then smoothly vanishes at $E_{\text{fast}}^l \approx 10$ GeV.

In contrast to this picture, the analogous spectrum of the less energetic signal leptons (plot *b*) starts sharply from zero and reaches a peak at $E_{\text{slow}}^l \approx 0.4$ GeV (where the spectrum of fast leptons only starts). Then it goes down and practically vanishes at the point $E_{\text{slow}}^l \approx 5$ GeV. One may see that the spectrum of slow leptons in a pair is more than by half shorter than that of fast leptons.

The difference between the P_T^l spectra of fast and slow leptons is not so large (see, correspondingly, Figs. 3, *a* and 3, *b*). They differ only by about 400 MeV shift to the left of

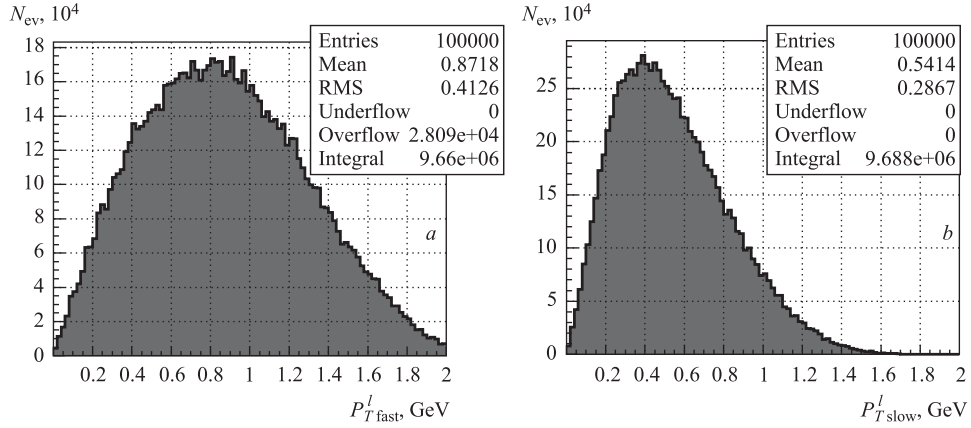


Fig. 3. Distribution of number of signal events versus the transverse momentum of signal leptons. *a*) The transverse momentum of fast leptons $P_{T\text{fast}}^l$; *b*) the transverse momentum of slow leptons $P_{T\text{slow}}^l$

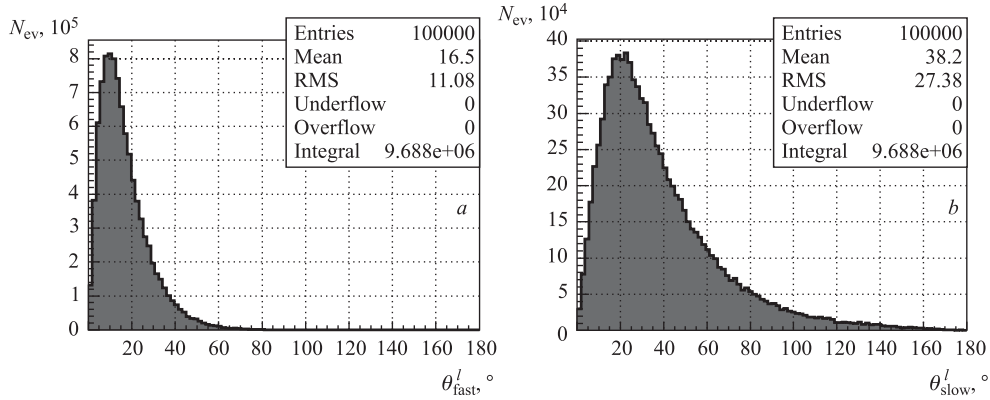


Fig. 4. Distribution of number of signal events versus polar (zenith) angle of signal leptons. *a*) The polar angle of fast leptons θ_{fast}^l ; *b*) the polar angle of slow leptons θ_{slow}^l

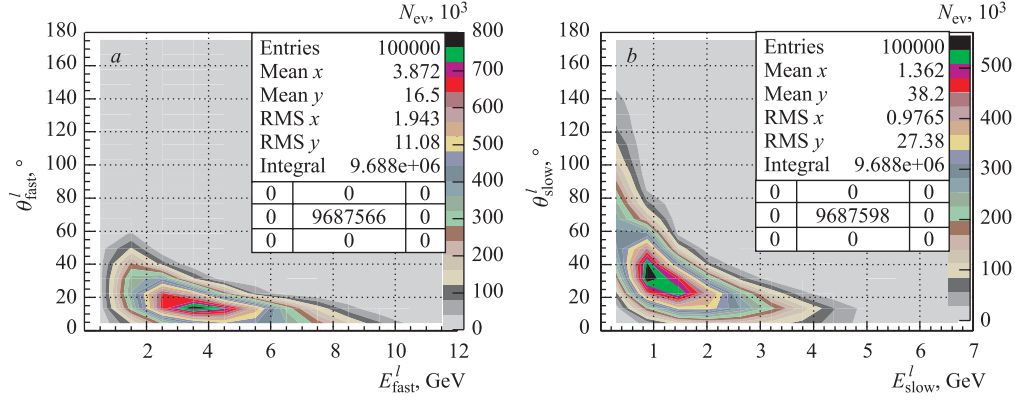


Fig. 5. Angle–Energy correlations. *a*) $\theta_{\text{fast}}^l/E_{\text{fast}}^l$ correlation for fast leptons; *b*) $\theta_{\text{slow}}^l/E_{\text{slow}}^l$ correlation for slow leptons

the peak position of the slow lepton spectrum. Both of these spectra demonstrate that the main part of slow and fast leptons has $P_T^l > 0.2$ GeV.

Figure 4 demonstrates that the polar (zenith) angle from the z axis directed along the beam line) spectrum of less energetic leptons θ_{slow}^l (plot *a*) is shifted to the higher values, as compared to the spectrum of fast leptons θ_{fast}^l (plot *b*). It is seen that the mean value of slow leptons angle $\langle \theta_{\text{slow}}^l \rangle = 38.2^\circ$ is more than twice the analogous mean value of fast leptons: $\langle \theta_{\text{fast}}^l \rangle = 16.5^\circ$. Thus, we conclude that all fast leptons fly in the forward direction ($\theta_{\text{fast}}^l < 80^\circ$) and their spectrum practically finishes at $\theta_{\text{fast}}^l = 60^\circ$ (plot *a*), while about 17% of slow leptons (plot *b*) have $\theta_{\text{slow}}^l > 60^\circ$. It is worth noting that about 5% of slow leptons may scatter into the back hemisphere.

Figure 5 includes the Angle–Energy correlation plots for fast $\theta_{\text{fast}}^l/E_{\text{fast}}^l$ (plot *a*) and slow $\theta_{\text{slow}}^l/E_{\text{slow}}^l$ (plot *b*) leptons in a pair. Figure 5, *a* demonstrates that the value of the polar angle

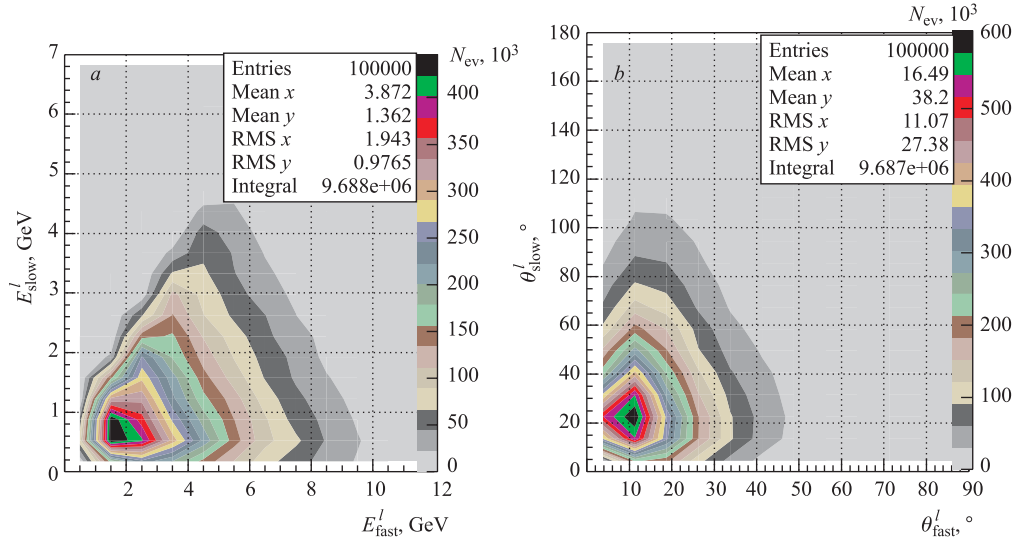


Fig. 6. *a*) Energy–Energy $E_{\text{slow}}^l/E_{\text{fast}}^l$ correlations; *b*) Angle–Angle $\theta_{\text{slow}}^l/\theta_{\text{fast}}^l$ correlations

θ_{fast}^l of fast leptons drops with the growth of their energy. Figure 5, *b* shows the kinematic region in θ – E plane which is covered by slow leptons.

After discussion of distributions of individual leptons let us turn to the distributions that characterize the produced pair of leptons as a whole system. Figure 6 shows the Energy–Energy $E_{\text{slow}}^l/E_{\text{fast}}^l$ (plot *a*) and Angle–Angle $\theta_{\text{slow}}^l/\theta_{\text{fast}}^l$ (plot *b*) correlations.

Data taking of searched signal events is strongly influenced by the cuts on lepton energies which are imposed from below to suppress the electronic noise and other detector effects which provide the instrumental background. The analysis of Fig. 6, *a* is summarized in Table 1. It demonstrates the loss of signal events after application of the cut $E_{\text{fast}}^l, E_{\text{slow}}^l \geq E_{\text{cut}}$ which sets the lower limit E_{cut} on the value of lepton energy.

Table 1. Efficiency of the $E_{\text{fast}}^l, E_{\text{slow}}^l \geq E_{\text{cut}}$

$E_{\text{cut}}, \text{GeV}$	The loss of signal events, %
0.5	24
1.0	45

The efficiency of collection of signal events which contain leptonic l^+l^- pairs depends on the angle coverage by the muon system or the EM calorimeter. Figure 6, *b* shows the Angle–Angle $\theta_{\text{slow}}^l/\theta_{\text{fast}}^l$ lepton correlation. The results of its analysis are given in Table 2, which demonstrates what part (in %) of signal events would be lost by imposing the upper limit θ_{cut} on the size of muon system or EC.

Table 2. Efficiency of the $\theta_{\text{slow}}^l, \theta_{\text{fast}}^l \leq \theta_{\text{cut}}$ cut

$\theta_{\text{slow}}^l, \theta_{\text{fast}}^l \leq \theta_{\text{cut}}, ^\circ$	The loss of signal events, %
20	80
40	39
60	17
90	5

The last line of Table 2 shows that even in the case that the muon system or the EM calorimeter would cover the angle region $\theta^l \leq 90^\circ$, about 5% of the events containing the l^+l^- signal pairs would be lost.

2. SOME LEPTON PAIR VARIABLES FOR THE $q\bar{q} \rightarrow \gamma^* \rightarrow l^+l^-$ SUBPROCESS

We consider here a set of physical variables which characterize a produced lepton pair as a whole system. These variables are constructed from the components of the total 4-momentum of initial-state quark–antiquark system $P_\alpha^{q\bar{q}} = P_\alpha^q + P_\alpha^{\bar{q}}$ ($\alpha = 0, 1, 2, 3$) and its analog $P_\alpha^{l^+l^-} = P_\alpha^{l^+} + P_\alpha^{l^-}$ for a lepton pair. Thus, Figs. 7, *a, b* show, correspondingly, the distributions of the invariant masses of initial-state quark–antiquark pair

$$M_{\text{inv}}^{q\bar{q}} = \sqrt{(P^{q\bar{q}})^2} = \hat{m}, \quad (1)$$

and the invariant mass of the final-state lepton–antilepton pair

$$M_{\text{inv}}^{l^+l^-} = \sqrt{(P^{l^+l^-})^2} = Q, \quad Q^2 = (P_\alpha^{l^+} + P_\alpha^{l^-})^2. \quad (2)$$

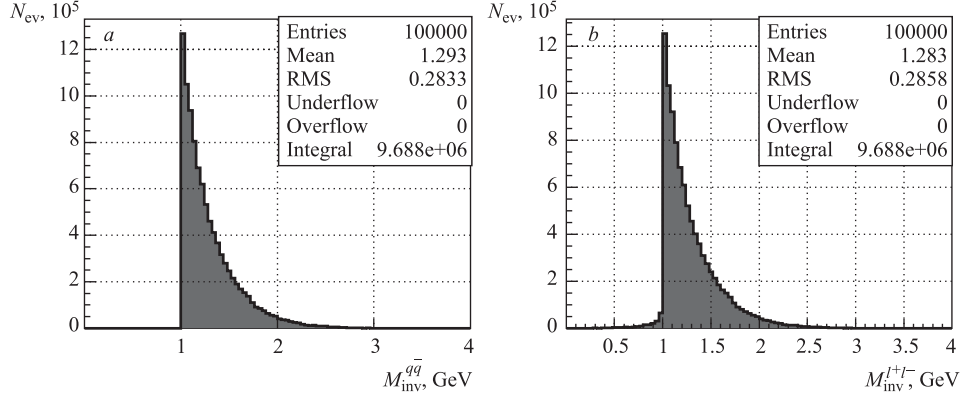


Fig. 7. Distribution of number of signal events versus the invariant mass. *a*) The invariant mass of initial-state quark–antiquark system $M_{\text{inv}}^{q\bar{q}}$; *b*) the invariant mass of final-state lepton–antilepton pair $M_{\text{inv}}^{l^+l^-}$

Both invariant mass distributions look rather similar. They are rather short and drop fastly. The distribution of the invariant mass $M_{\text{inv}}^{q\bar{q}}$ of the initial-state $q\bar{q}$ system sharply starts at the point $M_{\text{inv}}^{q\bar{q}} = 1$ GeV and finishes at $M_{\text{inv}}^{q\bar{q}} = M_{\text{inv}}^{l^+l^-} \approx 2.5$ GeV. Such behaviour at the left boundary point is due to the internal PYTHIA restriction on the lowest value of the invariant mass of the initial-state two-body system of any fundamental quark–parton $2 \rightarrow 2$ subprocess.

Different to the spectrum of the invariant mass of the initial-state $q\bar{q}$ system, the invariant mass $M_{\text{inv}}^{l^+l^-}$ of the final-state l^+l^- system has a very small tail at smaller than 1 GeV values $M_{\text{inv}}^{l^+l^-} < 1$ GeV (see Fig. 7, *b*) (this left tail of $M_{\text{inv}}^{l^+l^-}$ may appear due to the final-state radiation (FSR) of photons by the produced leptons).

The spectrum of the total lepton pair energy $E^{l^+l^-} = E^{l^+} + E^{l^-}$ is shown in Fig. 8, *a*. It is seen that the lepton pair total energy distribution is by about 2 GeV longer than the spectrum of the fast leptons energy E_{fast}^l (see Fig. 2, *a*).

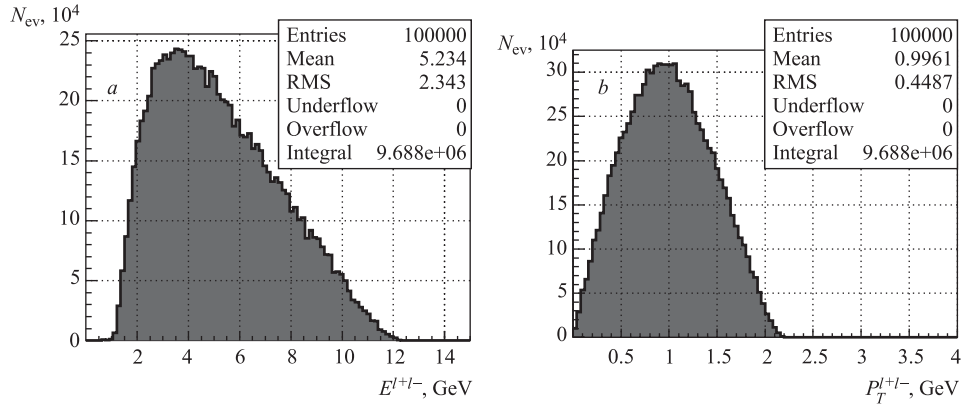


Fig. 8. Distribution of number of signal events versus: *a*) the total lepton pair energy $E^{l^+l^-}$; *b*) the total transverse momentum $P_T^{l^+l^-}$ of the lepton pair

The mean value of the total energy of the lepton pair, as seen from Fig. 8, *a*, is about 5 GeV. From the same plot of Fig. 8 it is clearly seen that in more than a half of events the lepton pair energy lays in the interval $4 \leq E^{l^+l^-} \leq 12$ GeV. So, one can conclude that the produced lepton pairs are rather energetic and they can carry away quite a noticeable part of the total energy of the colliding $\bar{p}p$ system.

The distribution of the longitudinal component $P_z^{l^+l^-} = P_z^{l^+} + P_z^{l^-}$ of the total 4-momentum of lepton pair system (not shown here) has a shape which is very similar to the energy $E^{l^+l^-}$ spectrum. The explanation of this fact follows from the shape of the distribution of the modulus of lepton pairs total transverse momentum

$$P_T^{l^+l^-} = |\mathbf{P}_T^{l^+l^-}| = |\mathbf{P}_T^{l^+} + \mathbf{P}_T^{l^-}|, \quad (3)$$

which is presented as $P_T^{l^+l^-}$ in Fig. 8, *b*. One may see that the transverse component distribution is much more narrow than that of the $E^{l^+l^-}$ and its mean value is about 1 GeV. For this reason, the main contribution to the value of lepton pair energy comes from the longitudinal component $P_z^{l^+l^-}$.

3. CUTS FOR BACKGROUND REDUCTION

To extract the information about the signal events, one needs to suppress the background contribution. The first type of the background are the «fake» leptons which originate from the hadronic decays at the same signal process¹.

It is found that the following cuts (applied to the sample of signal events):

- 1) we select the events with the only 2 leptons with $E_l \geq 0.2$ GeV, $P_{Tl} \geq 0.2$ GeV;
- 2) these 2 leptons must be of the opposite sign;
- 3) the vertex of lepton origin lies within the $R \leq 15$ mm from the interaction point, allow one to select a subsample of signal events including practically a negligible fraction of events containing fake leptons: 0.008% for the case of electron pair production and 0.001% for the muon pair production. The loss of the signal events due to application of cuts 1)–3) is shown in Table 3, from which one sees that it is possible to select the signal events which are almost free of background fake leptons at the cost of diminishing of the signal events sample by $\approx 14\%$ for e^+e^- and $\approx 17\%$ for $\mu^+\mu^-$ production.

Table 3. Loss of signal events after application of cuts 1)–3)

<i>N</i> of cuts	e^+e^- production, %	$\mu^+\mu^-$ production, %
1	14.330	16.525
1 & 2	14.340	16.805
1 & 2 & 3	14.341	17.108

¹For detailed distributions of such fake leptons see [6].

The other source of the background is the leptons produced in the minimum bias (low- P_T and single diffractive scatterings) events and QCD (mainly $q + g \rightarrow q + g$, $g + g \rightarrow g + g$ and $q + q' \rightarrow q + q'$) processes where the possibility of appearance of two (and more) leptons in the final state is very high. The generation of the sample of $2 \cdot 10^8$ $\bar{p}p$ inelastic scattering events was done by PYTHIA with the account of the contribution of minimum bias and QCD parton subprocesses, including the signal $q + \bar{q} \rightarrow l^+ + l^-$ subprocess. According to PYTHIA, the total cross section of $\bar{p}p \rightarrow X$ inelastic scattering is equal to 50.17 mb which is about 10^7 times higher than that of the signal $pp \rightarrow l^+l^- + X$ process based on the quark-antiquark annihilation $q + \bar{q} \rightarrow l^+ + l^-$ subprocess ($\sigma = 5.57 \cdot 10^{-6}$ mb).

Figures 9–14 include the plots which show the distributions of kinematic variables of background leptons originating from hadron decays in minimum bias and QCD events sample. All these distributions are obtained without application of any cuts.

Figure 9 includes the distributions of the number of final-state background decay leptons (N_{bkg}^e for electrons and N_{bkg}^μ for muons) which may be produced in a single inelastic $\bar{p}p \rightarrow$

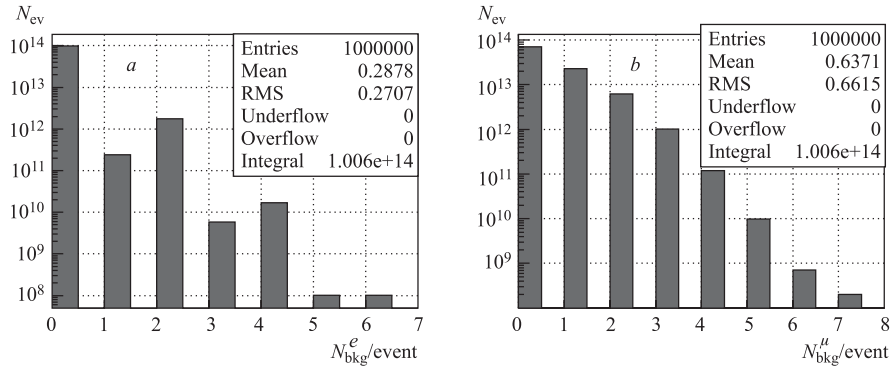


Fig. 9. Distribution of the number of final leptons per event in the background processes: a) electrons; b) muons

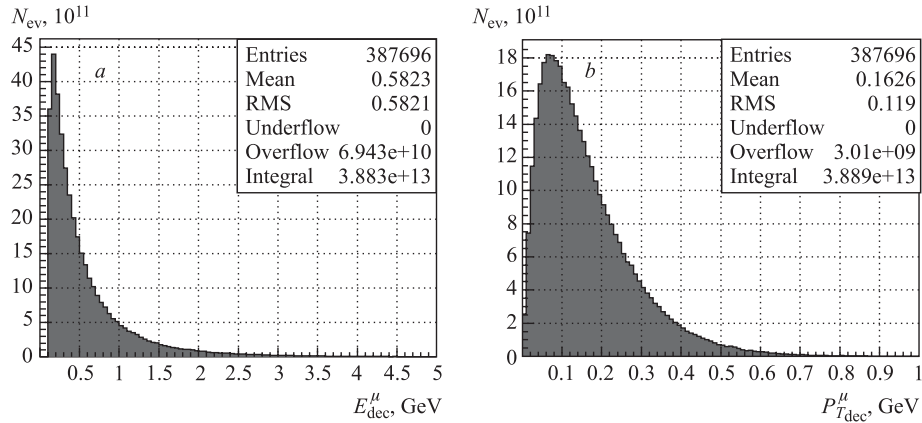


Fig. 10. Distribution of the background muons versus: a) E_{dec}^μ spectrum; b) $P_{T\text{dec}}^\mu$ spectrum

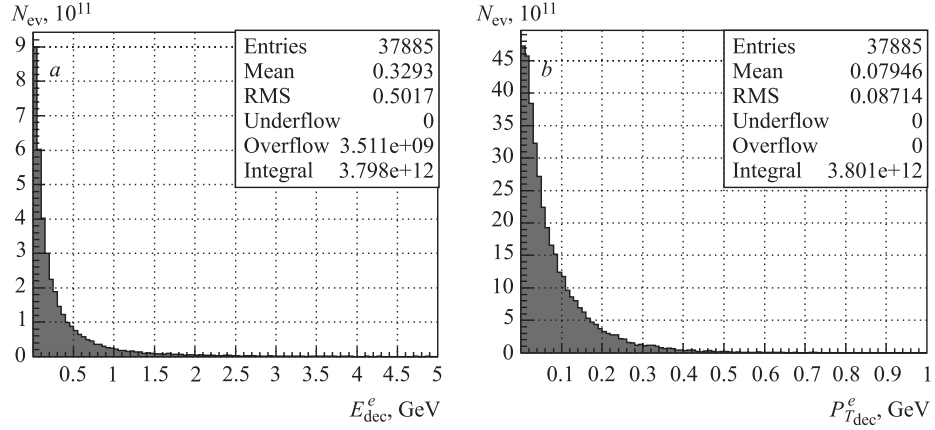
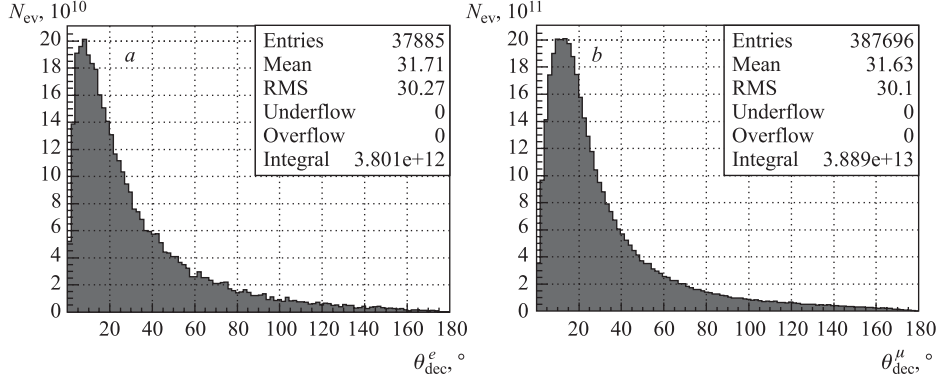

 Fig. 11. Distribution of the background electrons versus: a) E_{dec}^e spectrum; b) $P_{T\text{dec}}^e$ spectrum


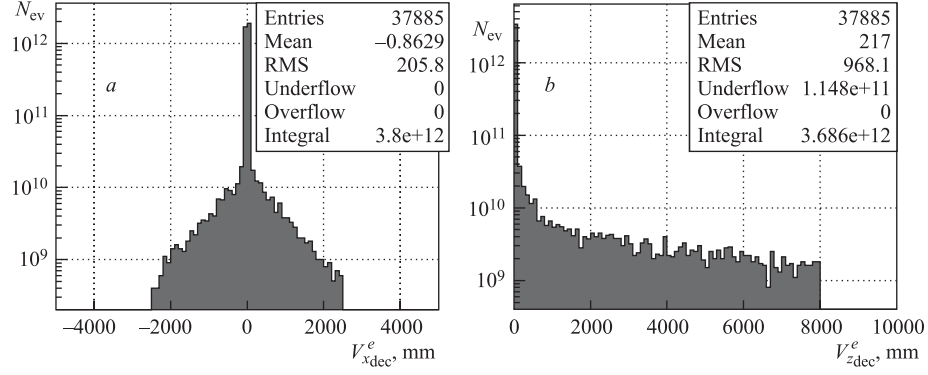
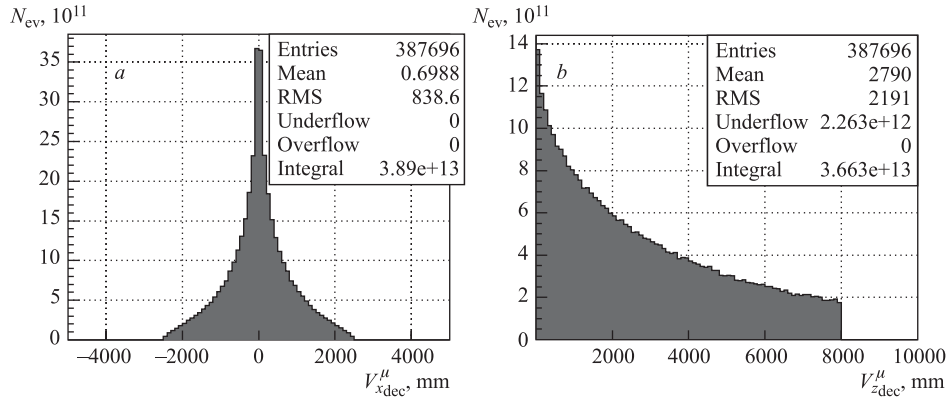
Fig. 12. Angle distribution of the background: a) electrons; b) muons

X event. One sees from Fig. 9, *a* that most of events ($\approx 96\%$) have no electrons at all. Analogously, it is seen from Fig. 9, *b* that the fraction of events without muons in the final state is about 60%.

The energy E_{dec} and transverse momentum $P_{T\text{dec}}$ spectra of the background decay leptons are presented in Fig. 10 for muons and in Fig. 11 for electrons. From Figs. 10, *b* and 11, *b* one sees that the cut $P_l \geq 0.2$ GeV (see cut 1) can kill most of e^+e^- background and about 70% of $\mu^+\mu^-$ background.

Figure 12 demonstrates the polar (zenith) angle θ_{dec} distributions of electrons (plot *a*) and muons (plot *b*). The shape of these distributions is very close to the shape of the polar angle distribution of slow leptons, θ_{slow}^l , shown in Fig. 4, *b*.

The distributions of lepton production vertices in the x - and z -plane are presented in Figs. 13 and 14 for the electrons and the muons, correspondingly. By comparing Fig. 13 with Fig. 14 one clearly sees the essential difference between the muon production vertex dis-

Fig. 13. Distribution of the background electron production vertices in the X plane (a) and Z plane (b)Fig. 14. Distribution of the background muon production vertices in the x plane (a) and z plane (b)

tribution and the analogous distribution of background electrons which are produced mostly very close to $\bar{p}p$ interaction point (see [6] for details).

To reduce background contribution from the minimum bias and QCD events, we added two new cuts to the previously used cuts 1)–3):

4) $M_{\text{inv}}(l^+, l^-) \geq 0.9 \text{ GeV}$;

5) lepton isolation criteria: the summed energy E_{sum} of all particles around the lepton within the cone of the radius $R = \sqrt{\Delta_\varphi^2 + \Delta_\eta^2} = 0.2$ in the $\eta - \varphi$ space is not higher than $E_{\text{sum}} \leq 0.5 \text{ GeV}$ ¹.

Here $\Delta_\varphi = \varphi_l - \varphi_p$ is the difference of the azimuth angles φ of the lepton (l) 3-momentum and the 3-momentum of the particle (p), contained in the cone around the lepton. Analogously, $\Delta_\eta = \eta_l - \eta_p$ is the difference of the lepton and the particle pseudorapidities.

¹The azimuth angle φ and the polar (zenith) angle Θ spherical coordinates are used to determine the direction of the 3-momentum of any particle. η is the particle pseudorapidity, defined by the formula $\eta = -\ln \text{tg}(\Theta/2)$ where Θ is the polar (zenith) angle.

The results of the sequent application of all five cuts to the sample of inelastic $\bar{p}p \rightarrow X$ events which includes the minimum bias and QCD events are collected in Table 4.

Table 4. Cuts influence for background events

N of cuts	S/B for $\mu^+\mu^-$ production	Efficiency	S/B for e^+e^- production	Efficiency
1	$1.41 \cdot 10^{-5}$	0.007	$5.34 \cdot 10^{-4}$	$1.78 \cdot 10^{-4}$
2	$2.12 \cdot 10^{-5}$	0.665	$5.41 \cdot 10^{-4}$	0.98
3	$9.94 \cdot 10^{-5}$	0.002	$5.47 \cdot 10^{-4}$	0.99
4	0.123	0.08	$9.27 \cdot 10^{-2}$	0.006
5	Background = 0	—	3.8	0.024

One can see from Table 4 that the last lepton isolation cut, i.e., the choice of only the events with the final-state leptons having the restricted value of the summarized energy (not greater than $E_{\text{sum}} = 0.5$ GeV) of other particles contained within the cone of some fixed radius $R = \sqrt{\varphi^2 + \eta^2} = 0.1, 0.2, 0.3 \dots$ around the direction of lepton momentum, allows one to achieve the value of signal-to-background ratio S/B = 3.8 in e^+e^- production case and to get rid completely of background in $\mu^+\mu^-$ case. In both cases the loss of signal events is about 8%.

Let us note that the same criteria, but with the use of a more restricted form of the forth cut $M_{\text{inv}}(e^+, e^-) \geq 1.0$ GeV, allow one to increase the signal-to-background ratio up to S/B = 9 in e^+e^- case at the cost of additional loss of 8% of the signal events.

4. REMARKS ON PHYSICS POTENTIAL OF LEPTON PAIR PRODUCTION PROCESSES

In addition to the opportunity, already mentioned in Introduction, of getting out the information about parton distributions, let us also mention here two other ones which may be useful for studying quark dynamics in proton and its PDFs.

The first one is connected with the processes of two

$$\bar{p}p \rightarrow l_1^+ l_1^- + l_2^+ l_2^- + X \quad (4)$$

or even three lepton pairs

$$\bar{p}p \rightarrow l_1^+ l_1^- + l_2^+ l_2^- + l_3^+ l_3^- + X \quad (5)$$

production in one event.

Both of them go through the quark annihilation $q\bar{q} \rightarrow l^+ l^-$ subprocesses and have smaller cross sections as compared to the $\bar{p}p \rightarrow l_1^+ l_1^- + X$ process. Nevertheless, they may contain interesting physical information which can be more easily extracted at an intermediate energy than at a high one. Thus, the measurement of the characteristics of the system of other than lepton pairs particles, produced in the process (4), shall give us the information about the

so-called «underlying» event, while the study of analogous distribution in the process (5) may give us the information about gluon content in the proton. The understanding of the physics of the «underlying» event, i.e., the interaction of partons which do not participate in the hard subprocess $q\bar{q} \rightarrow l^+l^-$, is very important for the interpretation of the results of the present Tevatron and future LHC experiments.

Another opportunity, provided by the processes (4) and (5) is the study of the so-called multiple parton interaction processes in pp and $p\bar{p}$ interactions which are also widely discussed in connection with the problem of a proper account of background contribution to the processes which are planned for studying the New Physics at Tevatron and LHC.

The third opportunity is connected with the possibility of measuring the characteristics of internal quark motion in the proton. This possibility is based on the fact that the shape of the distribution of the modulus of the vector sum of quark and antiquark transverse momentum vectors

$$P_T^{q\bar{q}} = |\mathbf{P}_T^{q\bar{q}}| = |\mathbf{P}_T^q + \mathbf{P}_T^{\bar{q}}| \quad (6)$$

practically coincides (due to the transverse momentum conservation law) with the shape of the above-considered distribution of the modulus of the lepton pair transverse momentum $P_T^{l^+l^-}$, shown in Fig. 8, ¹.

The variable $P_T^{q\bar{q}}$ is of special interest because it contains the information about two important physical features of quark dynamics inside the hadron. Indeed, in our case when a beam antiproton is directed along the z axis and it scatters over the proton fixed target, there may be only three sources of transverse motion of quarks in the initial state²:

A) The internal Fermi motion of quarks (with some transverse velocity) inside a proton, i.e., the so-called « k_T -effect»;

B) initial-state radiation (ISR) of gluons or photons from quarks before hard quark–antiquark annihilation;

C) final-state radiation (FSR) of photons from quarks after hard quark–antiquark annihilation.

Let us mention that the effect of the process C) is expected to be very small due to its electromagnetic nature as compared with the contribution from the first two A) and B) which are caused by strong interaction.

The importance of the first two effects A) and B) was recently discussed [8] in connection with the interpretation of prompt photon production study in the E706 experiment at Fermilab [9] and also with the study of « $\gamma + \text{jet}$ » events at the LHC [10] and Tevatron [11].

¹Recall (see Sec. 1) that all plots in Fig. 8 are done for the case that «Fermi motion» (or « k_T -effect») and ISR were switched «on».

²The values of transverse momenta of constituents in a target proton (which is at rest), as well as of those inside a beam antiproton (which moves along the z axis), are invariant under Lorentz transformations along the z axis.

CONCLUSION

The set of kinematic distributions are presented which allow one to estimate the energy, transverse momentum and angle ranges that may be covered by lepton pairs produced in quark–antiquark annihilation process. They may be useful for proper design of the muon system and the electromagnetic calorimeter for the detector of the PANDA experiment at FAIR.

It is also argued that a lot of interesting physical information about proton quark structure functions and quark dynamics (intrinsic Fermi motion of quarks inside the proton, multiple quark interactions, gluon content in the proton) can be extracted by the analysis of the corresponding future data of the PANDA experiment.

An important problem for this study is the estimation of the size of a possible background. The set of cuts are worked out here which may allow one to suppress effectively the background contribution. The account of the instrumental effects by the detector Monte-Carlo modeling would be the subject of the following publications.

The authors are grateful to G.D. Alexeev for the suggestion of this topic for study, the interest in the work and multiple stimulating discussions of the questions concerned.

REFERENCES

1. *Matveev V.A., Muradian R.M., Tavkhelidze A.N.* Muon Pair Production in Strong Interactions and Asymptotic Sum Rules. JINR Preprint P2-4543. Dubna, 1969. 23 p.; SLAC-TRANS-0098; JINR-P2-4543, June 1969. 27 p., translated from a Dubna preprint JINR-P2-4543 (1969).
2. *Drell S.D., Yan T.M.* Massive Lepton Pair Production in Hadron–Hadron Collisions at High Energies. SLAC Preprint SLAC-PUB-0755. 1970. 12 p.; Phys. Rev. Lett. 1970. V.25. P.316–320.
3. *Albajar C. et al. (CERN UA1 Collab.)* // Phys. Lett. B. 1988. V.209. P.397;
Gaughey P.L. et al. (FNAL E772 Collab.) // Phys. Rev. D. 1994. V.50. P.3038.
4. *Martin A.D. et al.* // Eur. Phys. J. C. 1998. V.4. P.463.
5. *PANDA Collab.* Strong Interaction Studies with Antiprotons. Technical Progress Report for PANDA; FESR-ESAC/Pbar/Technical Progress Report. GSI. 2005.
6. *Skachkova A.N., Skachkov N.B.* Monte-Carlo Simulation of Lepton Pair Production in $\bar{p}p \rightarrow l^+l^- + X$ Events at $E_{\text{beam}} = 14$ GeV. hep-ph/0506139. 2005.
7. *Sjostrand T.* // Comp. Phys. Commun. 1986. V.39. P.347;
Sjostrand T., Bengtsson M. // Comp. Phys. Commun. 1987. V.43. P.367.
8. *Apanasevich L. et al.* // Phys. Rev. D. 1999. V.59. P.074007; hep-ph/9808467;
Huston J. // Intern. J. Mod. Phys. A. 2001. V.16S1A. P.205–208.

9. *Apanasevich L. et al. (Fermilab E706 Collab.)* // Phys. Rev. Lett. 1998. V. 81. P. 2642–2645; hep-ex/9711017.
10. *Bandurin D. V., Konoplyanikov V. F., Skachkov N. B.* hep-ex/0207028. 2002.
11. *Bandurin D. V., Skachkov N. B.* D0-NOTE-3948. FNAL, 2002; hep-ex/0203003. 2002; Phys. Part. Nucl. 2004. V. 35. P. 66–106 (Fiz. Elem. Chast. At. Yadra. 2004. V. 35. P. 113–177); hep-ex/0304010.

Received on November 14, 2008.